JOURNAL OF MATERIALS SCIENCE 35 (2000) 5427–5432

Examination of the thermophysical bond of insert-molded PC/C fiber composites

C. W. EXTRAND*, S. BHATT
Entegris, 3500 Lyman Blvd., Chaska, MN 55318, USA
E-mail: chuck_extrand@entegris.com

The adhesive strength of a thermophysical bond between two polymers has been examined using fracture mechanics. Bimaterial composite specimens were constructed by injecting C fiber polyetheretherketone (PEEK) into a mold containing one-half of a polycarbonate (PC) dogbone. The resulting series specimens were notched at the interface and tested in tension. Adhesion of the two materials was reasonably good, as demonstrated by fracture surfaces that showed a mixture of PC and C fiber PEEK fragments. Interfacial fracture energy of the composite was approximately 1.5 kJ/m^2, which is comparable to the cohesive strength of amorphous commodity polymers. Variations in test speed (below the glass transition temperature of the two components, approximately 140°C) had no appreciable affect on stiffness or fracture energy. However, fracture energies decreased slightly as temperature increased.

1. Introduction

Although fracture toughness of polyetheretherketone (PEEK) composites has been widely discussed in the literature [1–7], PEEK composites constructed by insert molding with other engineering polymers have received little attention. Insert molding often involves molding a higher performance polymer, such as PEEK, on to a less expensive one. This approach provides an economical method of producing higher performance products at a reduced cost [8, 9]. In some cases, it is a good alternative to polymer blends.

An important feature in many insert-molded products is good adhesion between the materials. In this study, the adhesive strength of the interface between polycarbonate (PC) and C fiber PEEK has been examined using fracture mechanics. Composite tensile specimens were constructed by injecting C fiber PEEK into a mold containing one-half of a PC dogbone to create a thermophysical bond. The interface acts as a flaw or stress riser of unknown size. In order to perform a controlled measurement, notches were intentionally introduced into specimens, then notched samples were tested in tension. Effect of notch size, test speed and temperature were examined for the composite as well as the materials of construction (PC and C fiber PEEK).

2. Analysis

2.1. General mechanics

Tensile stresses, σ, were calculated using elongation force, F, divided by the undeformed cross-sectional area, A [10, 11],

$$\sigma = F/A. \tag{1}$$

Tensile strains, ε, were determined from sample elongation, ΔL, and its initial length, L,

$$\varepsilon = \Delta L/L. \tag{2}$$

Tensile moduli, E, were computed as stress over strain, where strains were small and the materials were linearly elastic ($\varepsilon < 0.01$),

$$E = \sigma/\varepsilon. \tag{3}$$

Velocity of elongation (crosshead speed), v, and initial sample length were used to estimate strain rate, ε',

$$\varepsilon' = v/L. \tag{4}$$

2.2. Mechanics of composite specimens

Fig. 1 shows the central portion of a series composite tensile specimen. The two materials have different tensile moduli (E_1 and E_2), where $E_1 < E_2$. Each segment has the same cross-sectional area and the same fractional length ($L_1/L = L_2/L = 1/2$). When load is applied, this composite sample deforms with the same average stress in each component. However, because the materials differ in stiffness, the individual components do not deform to the same extent. The stiffer material deforms less while softer material deforms more. As a result, the apparent stiffness of the composite specimen depends on the moduli of the individual components, E_1 and E_2, as [12–19]

$$E = \frac{2E_1E_2}{(E_1 + E_2)}. \tag{5}$$

2.3. Fracture mechanics

The adhesive strength of the interface and the component materials were determined using fracture

* Author to whom all correspondence should be addressed.

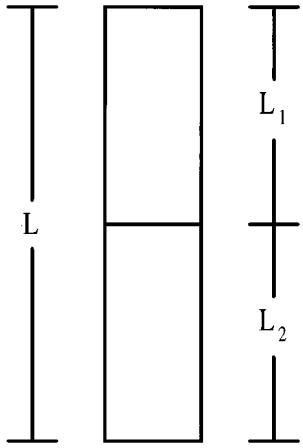

Figure 1 The central portion of a series composite specimen comprised of two materials with different tensile moduli, E_1 and E_2, where $E_1 < E_2$.

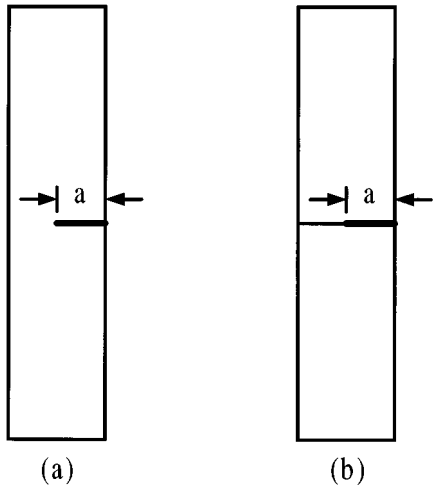

Figure 2 The central portion of tensile specimens with a single edge notch of length a. (a) monolithic specimen. (b) bimaterial composite with a notch at its interface.

mechanics. Fig. 2 shows tensile specimens with a single edge notch. The fracture energies, G, were calculated from the notch length, a, and the mechanical response of notched specimens as [20, 21]

$$G = 2.5\pi aU, \tag{6}$$

where U is the strain energy density to break (or area under the stress-strain curve). U was computed by integrating the stress-strain curve up to its breaking point,

$$U = \sigma(\varepsilon)\,\mathrm{d}\varepsilon. \tag{7}$$

If specimens broke at small strains with a linear stress-strain response, approximate values of fracture energy were estimated from breaking stresses, σ_b, as,

$$G^* = \frac{1.25\pi a\sigma_b^2}{E}. \tag{8}$$

3. Experimental

3.1. Materials

Polycarbonate (PC), C fiber polyetheretherketone (PEEK), and polystyrene (PS) were used to mold monolithic and bimaterial composite specimens. The C fiber PEEK compound contained <20% short C fiber.

3.2. Sample preparation

Bimaterial composites were fabricated by first molding PC dogbones and then cutting them in half with a bandsaw. Half pieces were inserted back into the dogbone mold and C fiber PEEK was injected.

Dogbones were notched at their midpoint for fracture energy measurements. For the composite specimens, this corresponded to placing the notch at the interface. Fig. 2 shows notch orientation. First, a scroll saw with 0.64 mm blade was used to cut within 0.5 mm of the desired depth. Then, a universal style utility blade was mounted in an INSTRON® 5582 test machine to cut the final 0.5 mm. A specimen was placed in the tensile tester and the blade was brought into contact with its edge near the notch. After resetting gauge length and centering the partially cut notch, the blade (crosshead) was moved downward at 2 mm/min until the preprogrammed notch length was reached. Notch length, a, was varied between 1 mm and 4 mm.

3.3. Mechanical testing

Samples were tested in tension using an INSTRON® 5582 test machine equipped with a 100 kN static load cell and extensometer. Gage length of the test machine was set at 115 mm. With the ASTM D638 Type 1 dogbones employed here, the effective gage length was $L \approx 100$ mm. Most samples were tested at 23°C using a crosshead speed of 2 mm/min ($\varepsilon' = 3 \times 10^{-4}$ s^{-1}). Alternatively, some were pulled at other speeds or temperatures to examine any potential rate or temperature effects. Five samples of each type were tested for yield stress, yield strain, breaking stress, breaking strain. Moduli and strain energy densities were determined from stress-strain curves. For notched samples, notch size, breaking stresses, moduli, and/or strain energy densities were used to calculate fracture energies. Averages and standard deviations were calculated for each specimen type.

3.4. Microbeam wide angle x-ray diffraction (MBWAXD)

Crystallinity and fiber orientation near the interface were examined by microbeam wide angle x-ray diffraction (MBWAXD) [22–24]. Samples were microtomed and then photographed using a matrixing microbeam x-ray camera mounted on a 12 kW Rigaku (RU 200B) rotating anode generator operated at 40 kV and 150 mA. The x-ray beam was monochromatized using a nickel foil.

This microbeam technique allows one to examine very small regions, with spatial resolution of 100 μm. Starting at the interface, x-ray photographs were taken along 100 μm steps, moving out normal from the interface into both the PC and the C fiber PEEK. The bulk and skin of C fiber PEEK was also examined by taking several x-ray photographs along a parallel line, three millimeters from the interface.

TABLE I Tensile properties of unnotched specimens

Material	σ_y (MPa)	ε_y (mm/mm)	σ_b (MPa)	ε_b (mm/mm)	E (GPa)
PC	60 ± 1	0.062 ± 0.001	66 ± 1	1.04 ± 0.01	2.3 ± 0.1
C fiber PEEK	NY	NY	129 ± 1	0.018 ± 0.001	12.0 ± 0.4
PC/C fiber PEEK	NY	NY	46 ± 8	0.013 ± 0.004	3.9 ± 0.2
PC/PC	NY	NY	33 ± 14	0.017 ± 0.009	2.5 ± 0.1

NY: No yield.

4. Results and discussion

4.1. Unnotched samples

Table I shows the tensile properties of unnotched specimens at room temperature. Properties for both PC and C fiber PEEK agreed well with literature values [25, 26]. Unnotched PC elongated about 6% before yielding with considerable necking; failure occurred at 90% elongation with a breaking stress of 66 MPa. C fiber PEEK elongated less than 2% before breaking at 130 MPa. It did not yield. For PC/C fiber PEEK composites, stress increased linearly with elongation; samples broke without yielding at $\varepsilon \approx 1.4\%$.

It is well known that interfaces can act as flaws or stress raisers. To demonstrate the effects of the interface on specimen strength, PC/PC composites samples were molded and tested. Results are included in Table I. Although modulus of the PC/PC composite was equal to that of single shot monolithic PC, the presence of the interface greatly reduced its strength. The overmolded PC/PC composite failed without yielding at 2% elongation, resulting in a 50% reduction in breaking stress.

Unnotched specimens were pulled at strain rates up to 8×10^{-2} s^{-1}. Variation in rate had little effect on the mechanical properties of the unnotched samples. Moduli were invariant. Stresses increased very slightly with increasing strain rate. Similar findings have been reported by other investigators [27].

Fig. 3 shows the relation between tensile modulus, E, and temperature, T, for the materials of construction and the composite. There was little change in stiffness for any of the specimens until temperatures reached the glass transition temperature (T_g) of the respective materials, about 140–150°C for both PC [28] and PEEK [29]. At higher temperatures, stiffness decreased dramatically for all specimens. Stiffness of the composite was dominated by PC. Modulus values calculated from Equation 5 agreed well with measured values.

4.2. Stress-strain behavior of notched samples

Fig. 4 shows a typical result for notched PC/C fiber PEEK composites. The stress-strain response was linear. Failure occurred abruptly at or near the interface. Fractures surfaces showed a mixture of PC and C fiber PEEK. Monolithic C fiber specimens behaved similarly. Stress increased linearly with strain, falling off slightly before breaking. On several occasions fragments were ejected as specimens broke.

Notched PC behaved differently. As notched PC samples were elongated, the material adjacent to the notch yielded and necked down. Stresses continued to climb slightly as the notch or crack began to grow. A 5% deviation in the compliance from an equivalent unnotched specimen was used to designate the initiation of crack growth in notched PC specimens [30].

4.3. Effect of notch size

In all cases, larger notches gave lower breaking stresses and breaking strains. Because the stress-strain behavior of monolithic C fiber PEEK and the PC/C fiber PEEK composite were more-or-less linear, it was possible to construct linear plots of breaking stress versus the inverse half power of the notch size ($a^{-1/2}$), shown in Figs 5 and 6. The points are experimental data. The solid lines represent linear regression that has been forced to pass through the origin. Using the slope of

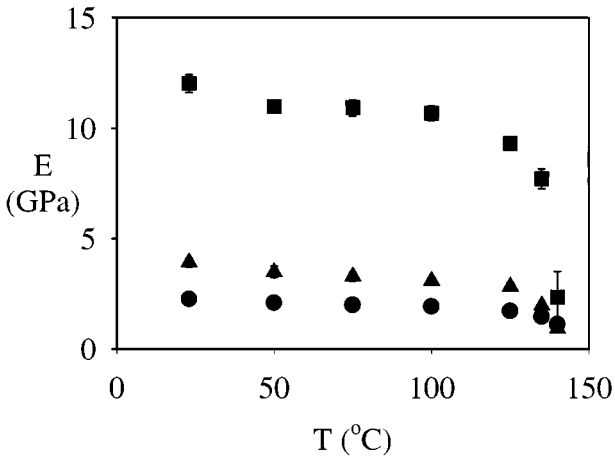

Figure 3 Tensile modulus, E, versus temperature, T, for unnotched monolithic PC, monolithic C fiber PEEK, and PC/C fiber PEEK composites ($T = 23\,^\circ$C, $\varepsilon' = 3 \times 10^{-4}$ s^{-1}). (●), monolithic PC; (■), monolithic C fiber PEEK; (▲), PC/C fiber PEEK composite.

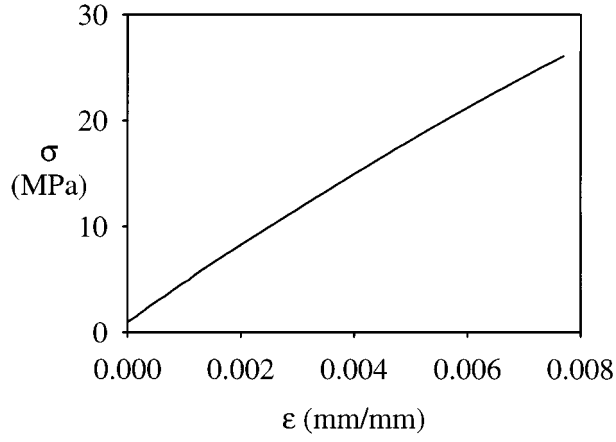

Figure 4 Stress, σ, versus strain, ε, for PC/C fiber PEEK composite with a 2 mm notch ($T = 23\,^\circ$C, $\varepsilon' = 3 \times 10^{-4}$ s^{-1}).

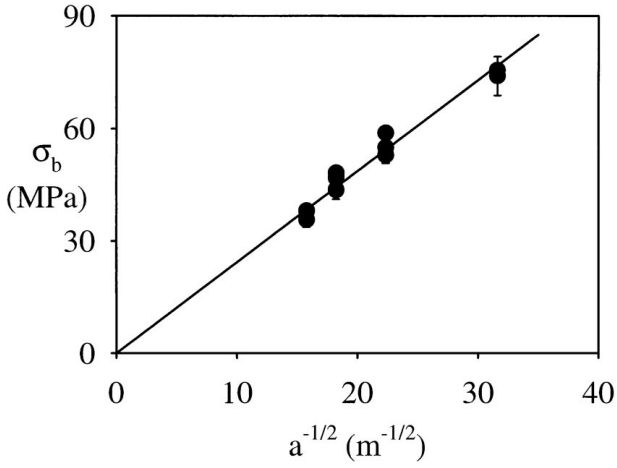

Figure 5 Breaking stress, σ_b, as a function of notch size, a, for monolithic C fiber PEEK ($T = 23\,^{\circ}$C, $\varepsilon' = 3 \times 10^{-4}$ s^{-1}).

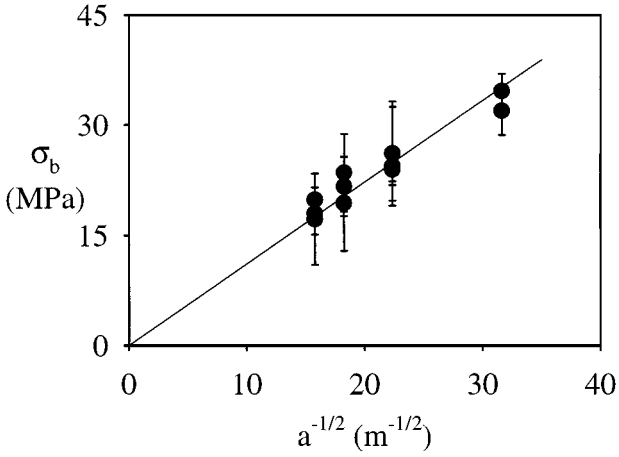

Figure 6 Breaking stress, σ_b, as a function of notch size, a, for the PC/C fiber PEEK composite ($T = 23\,^{\circ}$C, $\varepsilon' = 3 \times 10^{-4}$ s^{-1}).

these lines and the tensile moduli of unnotched samples in conjunction with Equation 8, fracture energies were determined to be $G^* = 2.0$ kJ/m^2 for monolithic C fiber PEEK and the $G^* = 1.2$ kJ/m^2 for PC/C fiber PEEK composite.

The non-linear fracture behavior of PC required a more general analysis. Strain energy densities were determined by integrating stress-strain curves up to the point of crack initiation, Equation 7, and then computing fracture energies, G, with Equation 6. Fig. 7 shows G values for PC with various notch lengths along with results for monolithic C fiber PEEK and the PC/C fiber PEEK composite. G values for PC were independent of notch length, $G = 8.5$ kJ/m^2.

Fracture energies are summarized in Table II for the materials of construction as well as their series composite. G values for monolithic PC and C fiber PEEK were in general agreement with values reported by other investigators [1, 2, 7, 31]. PC is a material known for its toughness. Thus, it's not surprising that it exhibited a fracture energy that is much greater than C fiber PEEK. Although the fracture behavior of the PC/C fiber PEEK composite was similar to monolithic C fiber PEEK, its fracture energy was lower. This was due, in part, to presence of the interface, which acts as a stress raiser. Nevertheless, the fracture energy of the PC/C fiber PEEK composite was comparable to amorphous commodity polymers such as PS or PMMA [18].

TABLE II Fracture energies at room temperature ($\varepsilon' = 3 \times 10^{-4}$ s^{-1})

Material	G (kJ/m^2)	G^* (kJ/m^2)
PC	8.5 ± 0.9	—
SP3000E	2.8 ± 0.3	2.0 ± 0.2
SP3000E/PC	1.6 ± 0.6	1.2 ± 0.5
PC/PC	3.1 ± 1.5	2.2 ± 0.4
PS	1.4 ± 0.3	1.2 ± 0.2

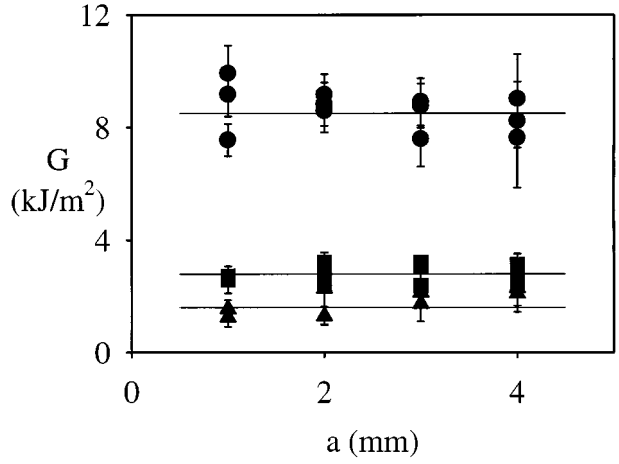

Figure 7 Fracture energy, G, versus notch size, a ($T = 23\,^{\circ}$C, $\varepsilon' = 3 \times 10^{-4}$ s^{-1}). (●), monolithic PC; (■), monolithic C fiber PEEK; (▲), PC/C fiber PEEK composite.

Results from the notched PC/PC composite further demonstrate the effect of an interface, Table II. They failed catastrophically without yielding, giving a much lower fracture energy than monolithic PC.

The larger variation observed in the breaking stresses, breaking strains, and fracture energies of the composite samples probably arose from a variety of sources: variation in the shape of the interface, notch location relative to the interface, as well as sample handling and placement. (The standard deviation for the unnotched PC/C fiber PEEK and PC/PC composite also was considerably larger than the unnotched monolithic specimens, Table I.)

4.4. Rate dependence of fracture energies

Monolithic and composite specimens with 2 mm notches were pulled at strain rates ranging from 2×10^{-5} s^{-1} to 8×10^{-2} s^{-1} ($v = 0.1$ mm/min to 500 mm/min) to undercover any potential rate effects. Fig. 8 shows fracture energy versus strain rate. No rate dependence was observed for the strain rates examined.

4.5. Temperature dependence of fracture energies

Fracture energies also were measured at temperatures as high as 140°C (approximately the onset of the glass-rubber transition for both PC and PEEK). Results are shown in Fig. 9. With increases in temperature, G

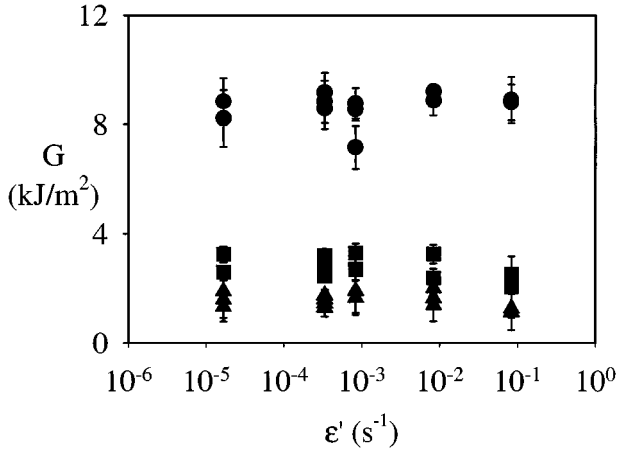

Figure 8 Fracture energy, G, versus strain rate, ε' ($T = 23\,^{\circ}$C, $a =$ 2 mm). (•), monolithic PC; (■), monolithic C fiber PEEK; (▲), PC/C fiber PEEK composite.

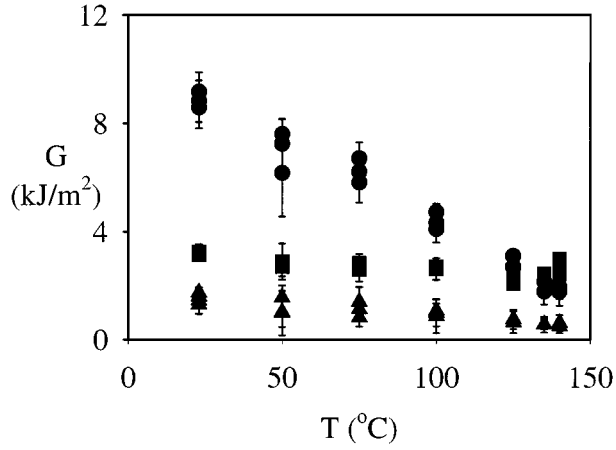

Figure 9 Fracture energy, G, versus temperature, T, for monolithic PC, monolithic C fiber PEEK, and PC/C fiber PEEK composites ($a = 2$ mm, $\varepsilon' = 3 \times 10^{-4}\ s^{-1}$). (•), monolithic PC; (■), monolithic C fiber PEEK; (▲), PC/C fiber PEEK composite.

values for PC dropped from 8 kJ/m^2 to less than 2 kJ/m^2 at 140°C. In accordance with previous work [32], the fracture energy for C fiber PEEK decreased only slightly with temperature. On the other hand, G values for PC/C fiber composites showed changes that were intermediate to those exhibited by the materials of construction, decreasing from 1.6 kJ/m^2 at room temperature to 0.5 kJ/m^2 at 140°C.

4.6. Morphology from MBWAXD

Crystallinity and fiber orientation of the PC/C fiber PEEK bimaterial composites were examined by MBWAXD analysis. PC near the interface was amorphous. The PEEK in the C fiber PEEK compound showed more interesting behavior. The bulk contained randomly oriented crystals. PEEK polymer near the PC interface and in the skin was amorphous. The amorphous layer at the interface was approximately 100 μm thick.

MBWAXD also revealed information regarding C fiber orientation in the C fiber PEEK compound. Even though the PEEK crystals in the bulk were randomly oriented, the C fiber of the bulk did show some alignment with the flow direction. Fiber orientation near the PC interface and in the skin was more pronounced – C fibers were strongly aligned parallel to the interface/surface.

5. Conclusions

Bimaterial composites failed at or near the interface. Fracture surfaces showed a mixture of PC and C fiber PEEK, suggesting good adhesion. Fracture energies of the composites were less than the materials of construction, yet indicated a reasonably strong adhesive bond. The strength of the adhesive bond of PC/C fiber PEEK composite is comparable to the cohesive strength of amorphous commodity polymers, such as PS or PMMA. Variations in test speed had little affect on stiffness or fracture energy. Fracture energies, however, did decline slightly with increasing temperature.

Acknowledgements

The authors wish to thank Entegris management for allowing the publication of this work. Also, thanks to G. Smith and T. Raser for molding of the test specimens, as well as J. McPhee and B. Wold for assistance in the mechanical testing. MBWAXD was performed in Prof. M. Cakmak's laboratory at The University of Akron.

References

1. P. J. HINE, B. BREW, R. A. DUCKETT and I. M. WARD, *Composite Sci. Tech.* **33** (1988) 35.
2. S. HASHEMI, A. J. KINLOCH and J. G. WILLIAMS, *J. Composite Materials* **24** (1990) 918.
3. C. Y. BARLOW, J. A. PEACOCK and A. H. WINDLE, *Composites* **21** (1990) 383.
4. G.-M. WU and J. M. SCHULTZ, *Polym. Composites* **11** (1990) 126.
5. H. MOTZ and J. M. SCHULTZ, *J. Thermoplastic Composite Materials* **3** (1990) 110.
6. J. KARGER-KOCSIS, *Polym. Bull.* **27** (1991) 109.
7. B. R. K. BLACKMAN, J. P. DEAR, A. J. KINLOCH, H. MACGILLIVRAY, Y. WANG, J. G. WILLIAMS and P. YAYLA, *J. Mat. Sci.* **30** (1995) 5885.
8. J. DE GASPARI, *Plastics Technology* **44** (1992) 44.
9. H. H. KAUSCH, "Advanced Thermoplastic Composites" (Hanser, New York, 1993).
10. I. M. WARD, "Mechanical Properties of Solid Polymers" (Wiley, New York, 1983), 2nd ed.
11. J. M. GERE and S. P. TIMOSHENKO, "Mechanics of Materials" 2nd ed. (PWS-Kent Publishing, Boston, 1984),
12. M. L. WILLIAMS, *Bull. Seism. Soc. Am.* **49** (1959) 199.
13. G. C. SIH and J. R. RICE, *J. Appl. Mech.* **31** (1964) 477.
14. F. ERDOGAN, *ibid.* **32** (1965) 403.
15. J. R. RICE and G. C. SIH, *ibid.* **32** (1965) 418.
16. V. L. HEIN and F. ERDOGAN, *Int. J. Fracture Mech.* **7** (1971) 317.
17. G. P. ANDERSON, S. J. BENNETT and K. L. DEVRIES, "Analysis and Testing of Adhesive Bonds" (Academic Press, New York, 1977).
18. S. WU, "Polymer Interface and Adhesion" (Marcel Dekker, New York, 1982).
19. C. W. EXTRAND and S. BHATT, *J. Appl. Polym. Sci.* **76** (2000) 1777.
20. A. A. GRIFFITH, *Phil. Trans. Royal Soc.* **A211** (1920) 163.
21. J. G. WILLIAMS, "Fracture Mechanics of Polymers" (Wiley, New York, 1987).
22. C. M. HSIUNG and M. CAKMAK, *J. Appl. Polym. Sci.* **47** (1993) 125.
23. *Idem., ibid.* **47** (1993) 149.

24. Y. ULCER, M. CAKMAK and C. M. HSIUNG, *ibid.* **55** (1995) 1241.
25. H. SAECHTLING, "Plastics Handbook" 2nd ed. (Oxford University Press, New York, 1992).
26. "International Plastics Selector, Vol. 2," 17th ed. (D.A.T.A. Business Publishing, Englewood, CO, 1996).
27. N. D. ALBÉROLA, P. MÉLÉ and C. BAS, *J. Appl. Polym. Sci.* **64** (1997) 1053.
28. J. BRANDRUP and E. H. IMMERGUT, (eds.), "Polymer Handbook" 3rd ed. (Wiley, New York, 1989).
29. D. J. BLUNDELL and B. N. OSBORN, *Polymer* **24** (1983) 953.
30. J. G. WILLIAMS and M. J. CAWOOD, *Polym. Testing* **9** (1990) 15.
31. A. KIM, C. P. BOSNYAK and A. CHUDNOVSKY, *J. Appl. Polym. Sci.* **51** (1994) 1841.
32. J. KARGER-KOCSIS and K. FRIEDRICH, *Polymer* **27** (1986) 1753.

Received 24 June 1999
and accepted 15 March 2000